



MIDDLE EAST TECHNICAL UNIVERSITY

EE568 Selected Topics On Electrical Machines

*Project Report: Torque in a Variable Reluctance
Machine*

M. Samet YAKUT

ID: 2305647

GitHub: `sametyakut`

DEPARTMENT OF ELECTRICAL & ELECTRONICS ENGINEERING

April 16, 2022

1 Introduction

Throughout this project assignment, a basic reluctance machine will be analyzed. At first, analytical modelling will be examined. The reluctance, inductance and torque equations will be derived. Afterwards, analysis will be conducted on a finite element analysis (FEA) software both with linear and nonlinear materials. Finally, results will be discussed.

2 Analytical Modelling

In the first part of the project, we are asked to analytically calculate the maximum and minimum reluctance and inductance. Furthermore, it is also asked to calculate the inductance as a function of rotation. Finally, torque will be calculated in this part.

2.1 Calculation of Maximum and Minimum Reluctance (and Inductance)

If we look closer to the machinery, we can see that the maximum air gap between the rotor and core is 2.5 mm in both sides of the rotor. On the other hand, minimum air gap distance is 0.5 mm in both sides. Since the core is infinitely permeable, the only reluctance is due to the air gap. The reluctance can be calculated as $R = \frac{l}{\mu_0 A_c}$, where l is the length of the air gap, μ_0 is the permeability of the air and A_c is the cross-sectional area.

The relation between reluctance and inductance is $L = N^2/R$.

Case-I: Calculation of maximum reluctance, and hence, minimum inductance.

To simplify the calculations, following assumptions are made.

- The cross-sectional area is uniform
- The cross-sectional area is rectangular with 15 mm width and 20 mm height

Thus, the $l = 5 \text{ mm}$, $A_c = 15\text{mm} \times 20\text{mm} = 300 \text{ mm}^2$, and $\mu_0 = 4\pi \times 10^{-7}$. Therefore, maximum reluctance and minimum inductance are

$$R_{max} = \frac{l}{\mu_0 A_c} = \frac{5 \times 10^{-3}}{300 \times 10^{-6} \times 4\pi \times 10^{-7}} = 1.32 \times 10^7 \text{ A.turns/Wb} \quad (1)$$

$$L_{min} = \frac{N^2}{R_{max}} = \frac{250^2}{1.32 \times 10^7} = 4.71 \text{ mH} \quad (2)$$

Case-II: Calculation of minimum reluctance, and hence, maximum inductance.

Minimum reluctance and maximum inductance can be calculated by making the same

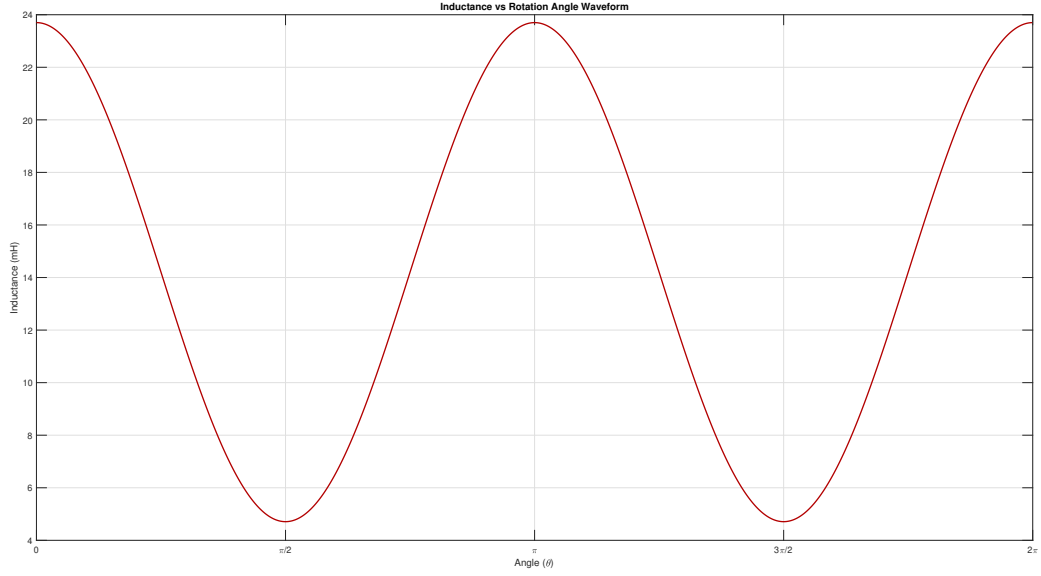


Figure 1: Inductance variation with rotation.

assumptions. The only difference is the value of the air gap length. Now, air gap length $l = 1 \text{ mm}$. Then,

$$R_{min} = \frac{l}{\mu_0 A_c} = \frac{1 \times 10^{-3}}{300 \times 10^{-6} \times 4\pi \times 10^{-7}} = 2.64 \times 10^6 \text{ A.turns/Wb} \quad (3)$$

$$L_{max} = \frac{N^2}{R_{min}} = \frac{250^2}{2.64 \times 10^6} = 23.7 \text{ mH} \quad (4)$$

2.2 Inductance with respect to Rotation Angle

It is known that frequency of inductance change is double of rotation frequency. Hence, inductance change with respect to rotation angle (θ) can be modeled as follows, and graph of variation can be seen in Fig. 1.

$$L(\theta) = \frac{L_{max} + L_{min}}{2} + \frac{L_{max} - L_{min}}{2} \cos(2\theta) \quad (5)$$

$$L(\theta) = 14.205 \times 10^{-3} + 18.99 \times 10^{-3} \cos(2\theta) \quad (6)$$

Note that θ is defined as 0 at the position where air gap is minimum.

2.3 Derivation of Torque

The relation between the torque and inductance is

$$T(\theta) = \frac{1}{2} I^2 \frac{dL(\theta)}{d\theta} \Big|_{i=\text{constant}} \quad (7)$$

$$T(\theta) = 0.17\sin(2\theta) \quad (8)$$

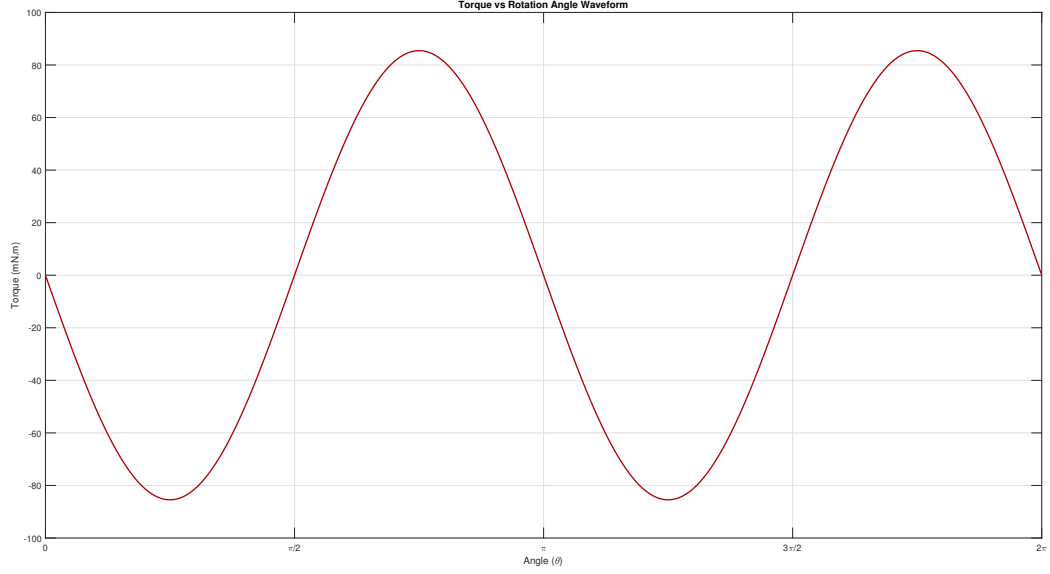


Figure 2: Torque waveform with respect to rotation angle

2.4 Including the Nonlinear Effects

FEA software can be a good choice for including the nonlinear effects such as fringing flux and nonhomogenous flux distribution. For leakage and fringing fluxes, different paths can be selected for Ampere's Circuital Law. In other words, different paths with the different number of turns or different sizes can be selected to obtain the leakage or fringing flux more accurately. Moreover, to include the effect of nonhomogenous flux distribution,

3 FEA Modelling (2D - Linear Materials)

After drawing the system in Maxwell 2D, copper is assigned for coils. The core material is selected as "steel 1010" from the system library; however, it was nonlinear. To linearize this material, I cloned the steel 1010 and created my linear B-H curve for this clone, i.e., the material property is changed to simple with a relative permeability of 667.75. Then, I assigned this new and purely linear material to the core. Long story short, the core material is the linearized version of steel 1010. The flux density plots can be seen below.

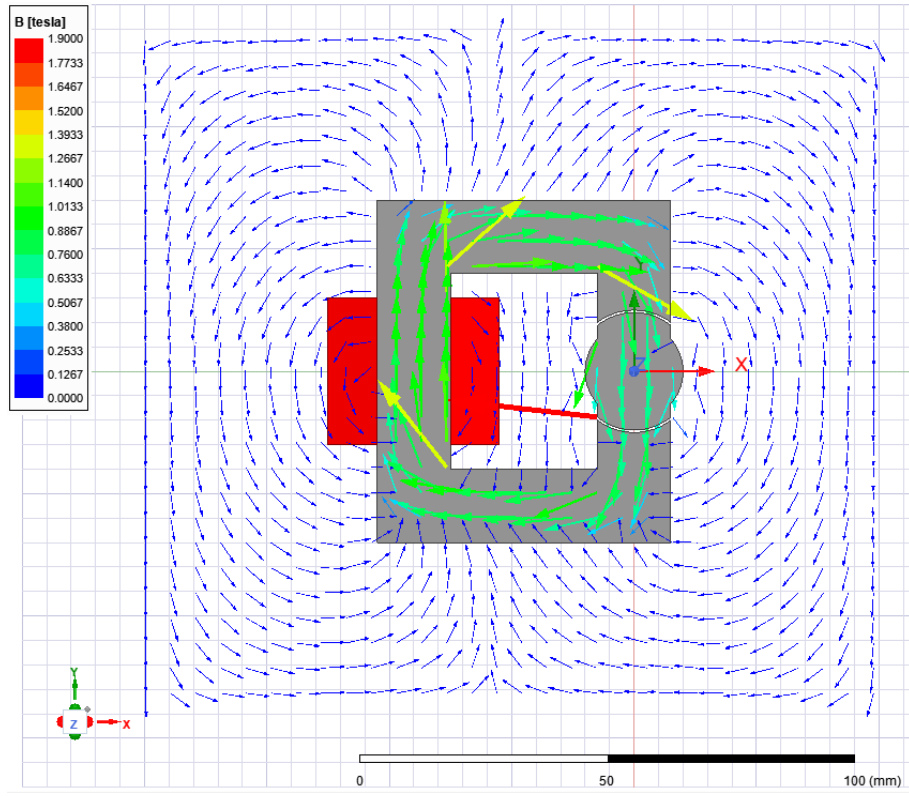


Figure 3: Magnetic field intensity of linear material for $\theta = 0^\circ$

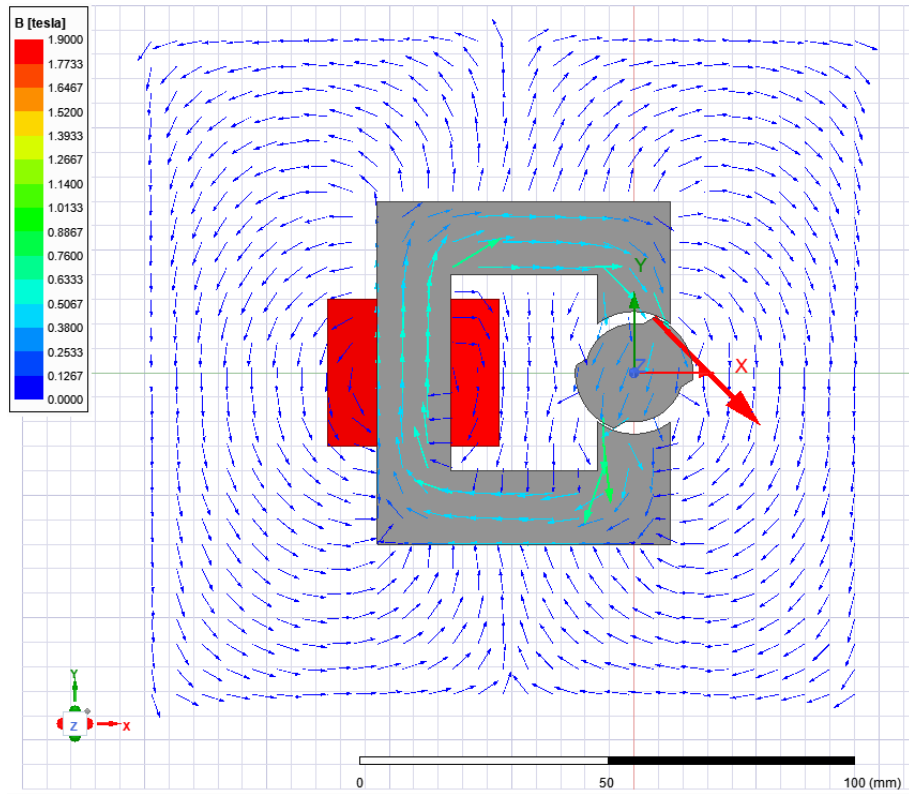


Figure 4: Magnetic field intensity of linear material for $\theta = 45^\circ$

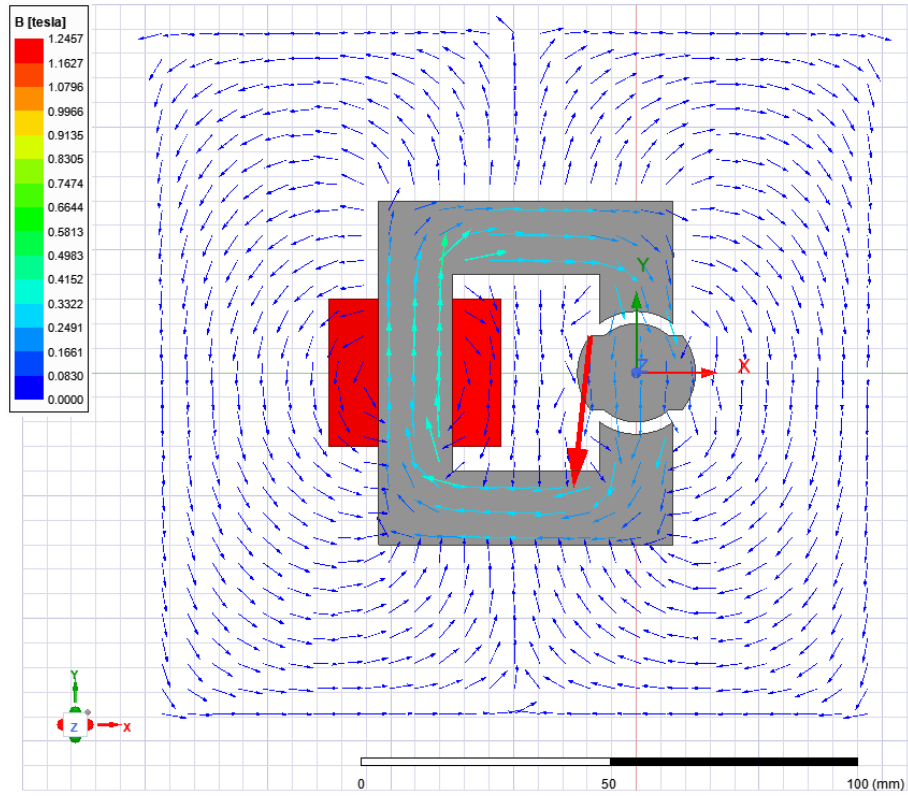


Figure 5: Magnetic field intensity of linear material for $\theta = 90^\circ$

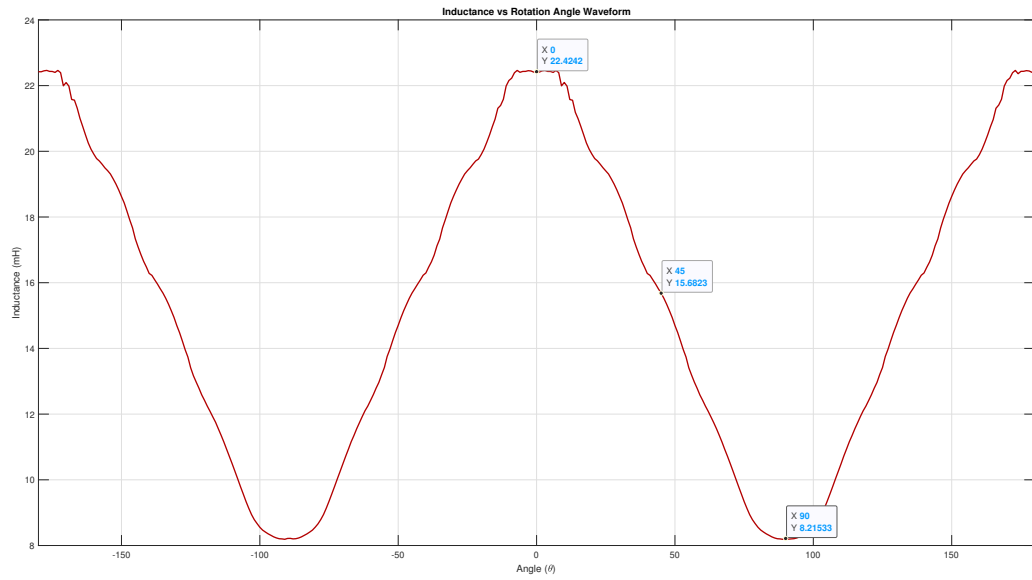


Figure 6: Inductance variation with rotation (FEA)

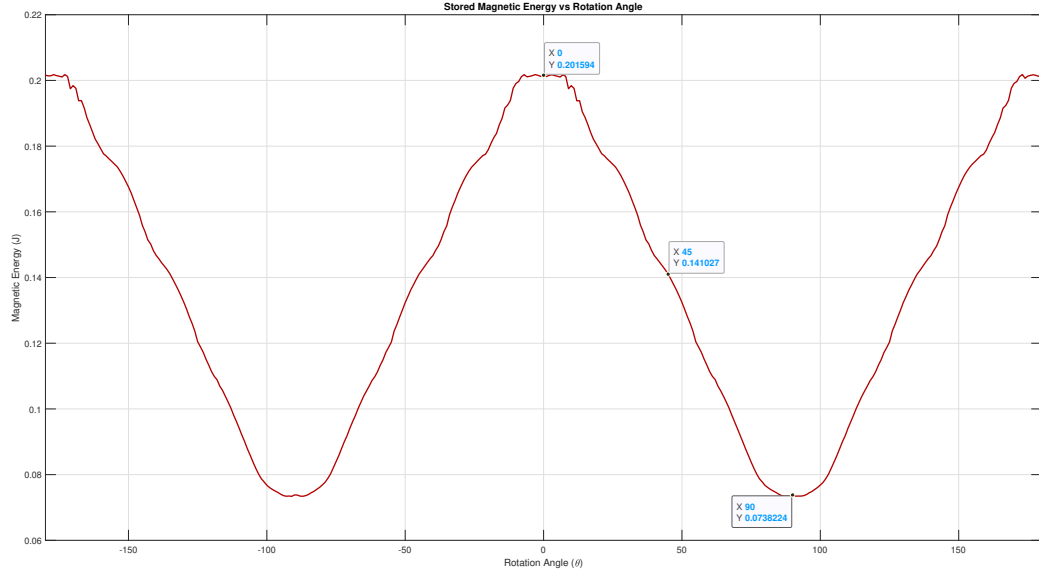


Figure 7: Total stored magnetic energy variation with rotation (FEA)

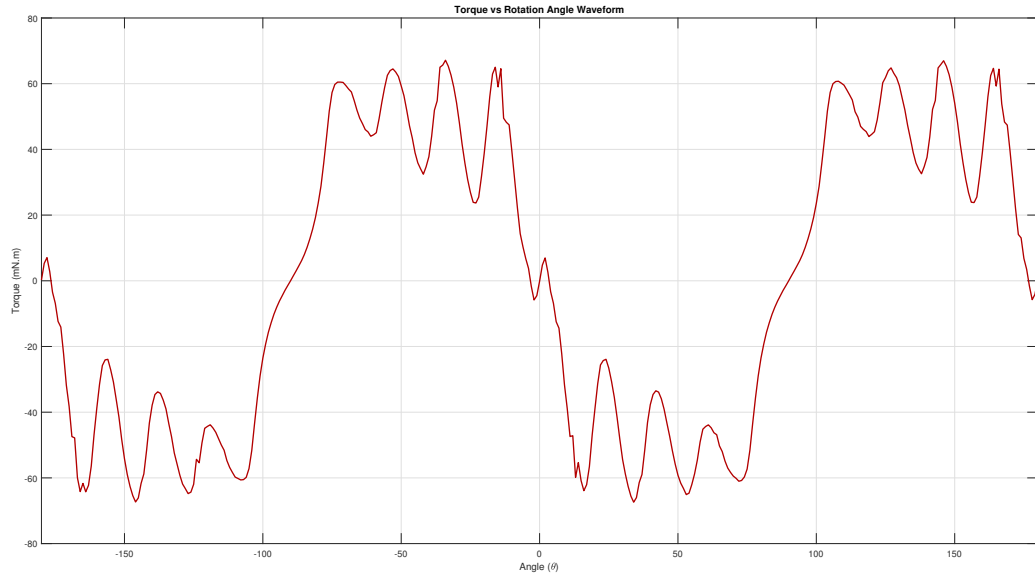


Figure 8: Torque variation with rotation (FEA)

Note that there are deviations between FEA and analytical models because during the analytical modelling, it is assumed that flux distribution is homogenous, and there is no flux fringing. Moreover, it is assumed to core to be infinitely permeable, i.e., zero reluctance. However, these are not the cases in reality. So, the FEA model gives the more accurate result since it does not make these assumptions.

4 FEA Modelling (2D - Nonlinear Materials)

Other than linear modelling, original version of "*Steel 1010*" from system library is used. The same model is also analyzed with nonlinear material. Magnetic field intensity vector, inductance, stored magnetic energy and torque with respect to rotation angle plots are presented below.

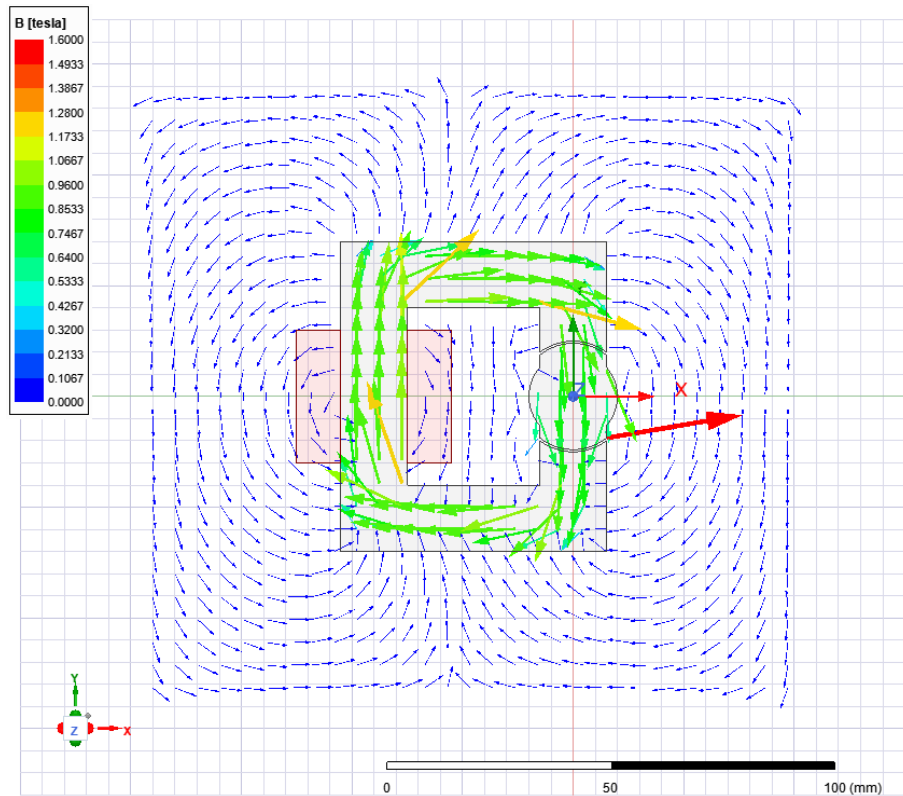


Figure 9: Magnetic field intensity of nonlinear material for $\theta = 0^\circ$

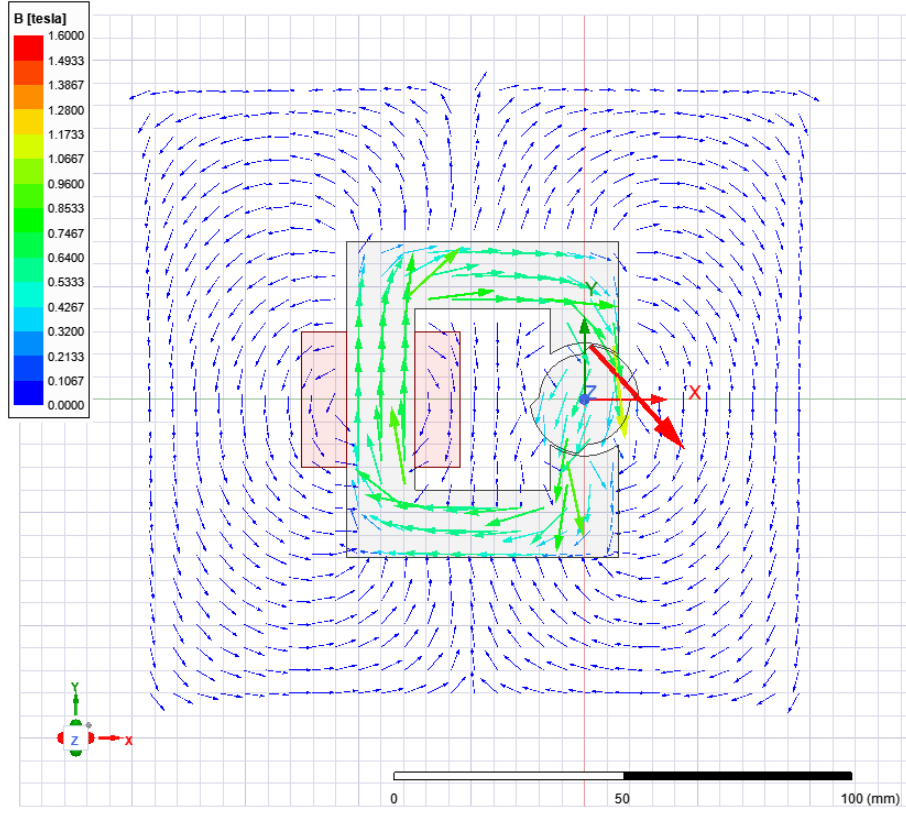


Figure 10: Magnetic field intensity of nonlinear material for $\theta = 45^\circ$

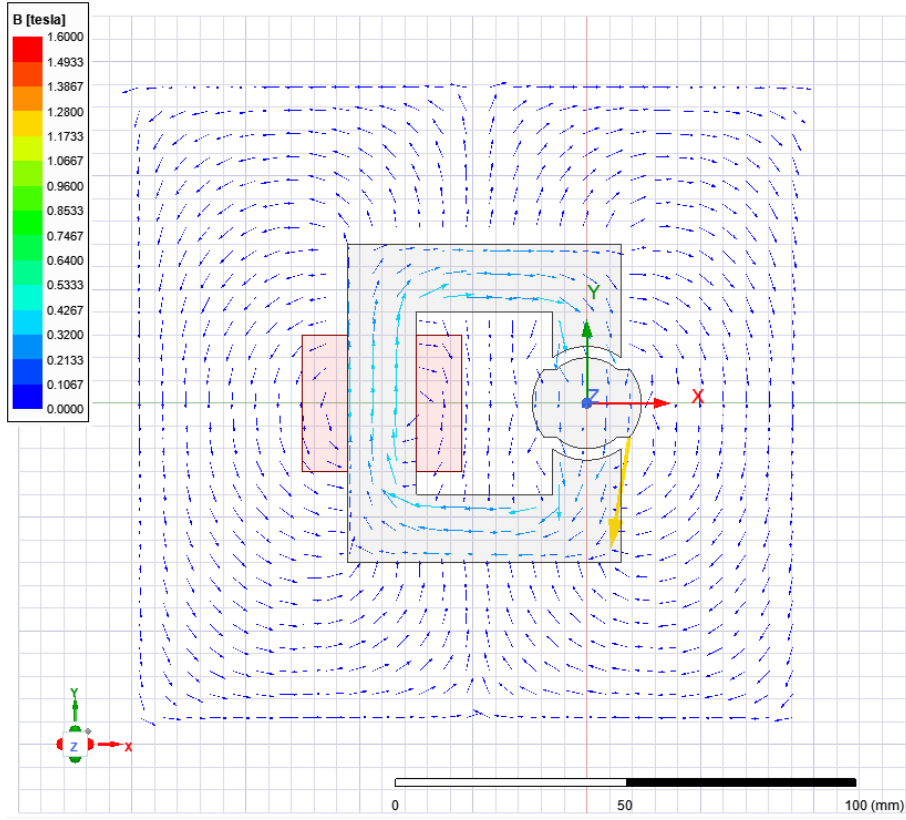


Figure 11: Magnetic field intensity of nonlinear material for $\theta = 90^\circ$

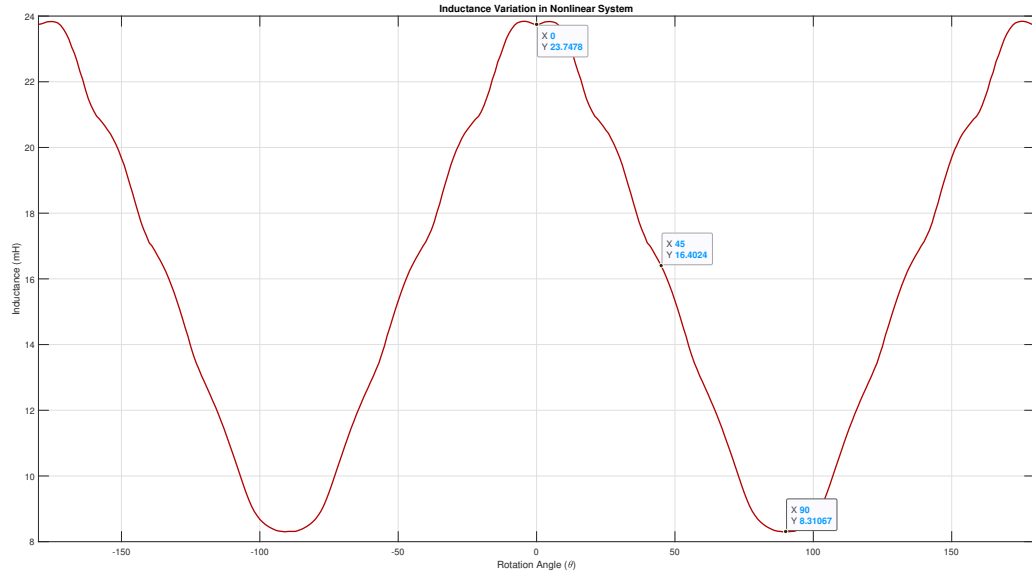


Figure 12: Inductance change in nonlinear system model

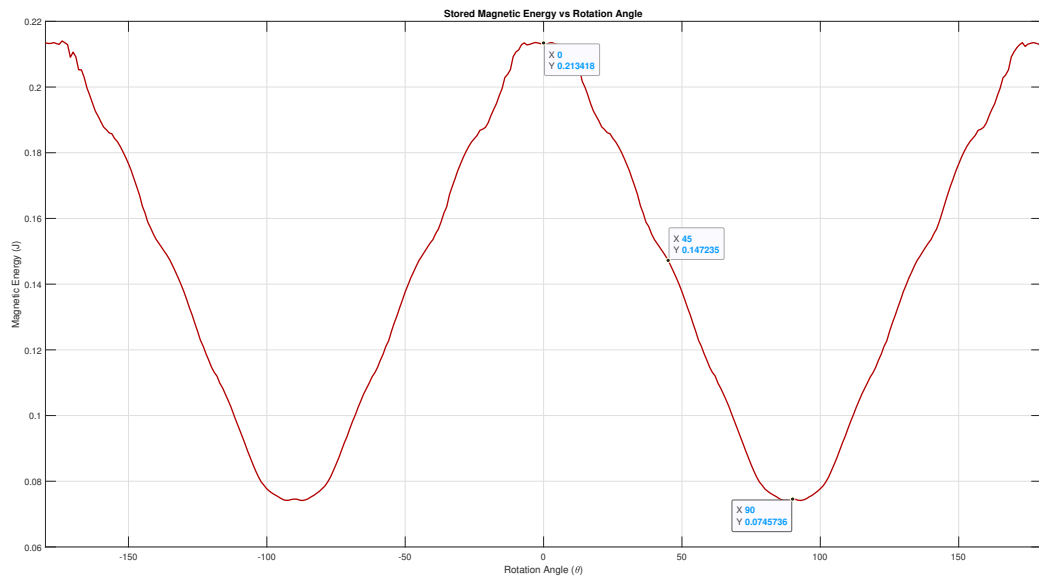


Figure 13: Total stored magnetic energy in nonlinear system model

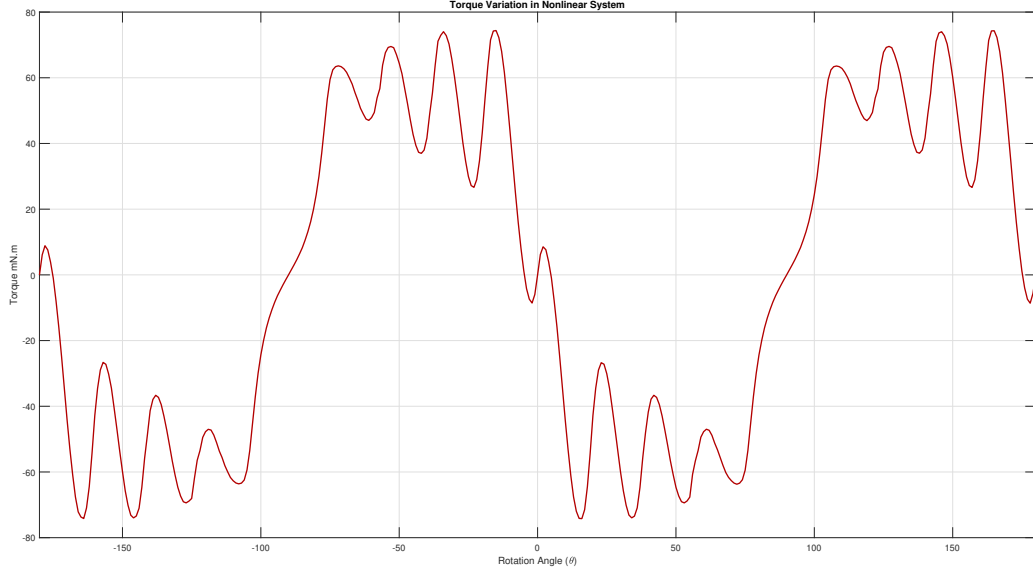


Figure 14: Torque change in nonlinear system model

It can be easily seen from the results that the peak value of the inductance is slightly larger than the linear FEA model. In other words, nonlinear effects caused the increase in inductance value at its maximum point. More technically, once the core saturates, inductance drops. However, the saturation point of *steel 1010* is larger than the magnetic field intensity throughout the core, which can also be seen in the vector plots. Hence, saturation is not observed at all, i.e., some points of the core saturates not all of it. On the other hand, the fringing flux increases the cross-section area that flux moves, which in turn decreases the reluctance. So, inductance increases. To sum up, since the material is not saturated at all, inductance is slightly increased due to the effect of fringing flux. In terms of stored magnetic energy, it is seen that energy is slightly increased in nonlinear modelling, which is expected. In other words, energy is increased due to rising area of the left hand side of the nonlinear B-H curve.

5 Control Method

It can be seen from the **animations** that rotor oscillates, not rotates continuously. To overcome this, a square wave can be applied to prevent from the rotor oscillating. In more detail, when the rotor passes through the core, the square wave will be inactive to prevent from supplying torque in the reverse direction. Hence, rotor will continuously rotate. Analytically, if the input current is negative between rotation angles 0 and $\pi/2$, and π and $3\pi/2$, then the only positive torque will be generated, check Fig. 2. Implying a basic version of it, i.e., supplying only positive and zero current depending on the position gives the following waveforms.

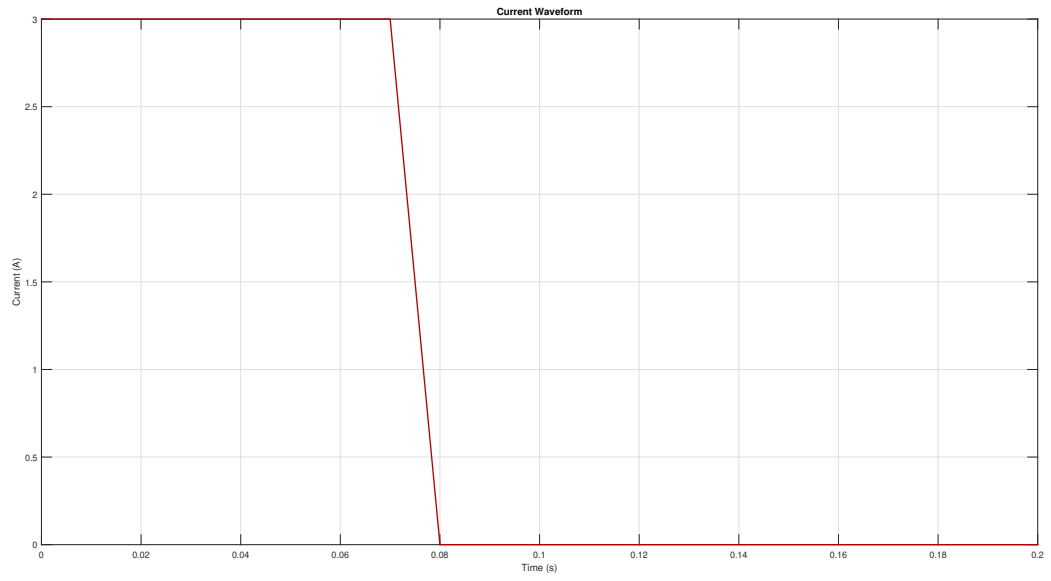


Figure 15: Current in controlled continuous rotation of linear system

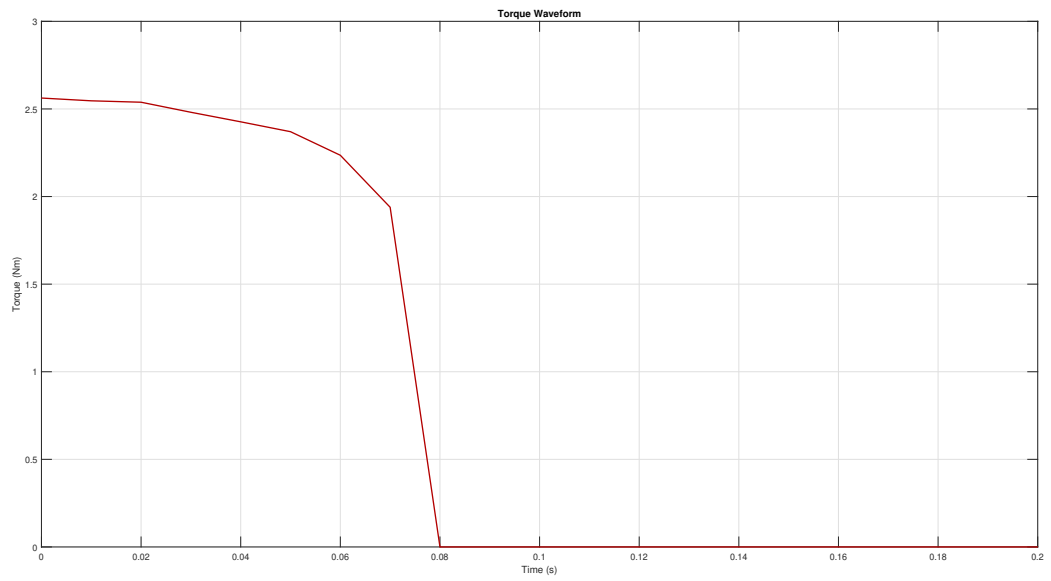


Figure 16: Torque in controlled continuous rotation of linear system

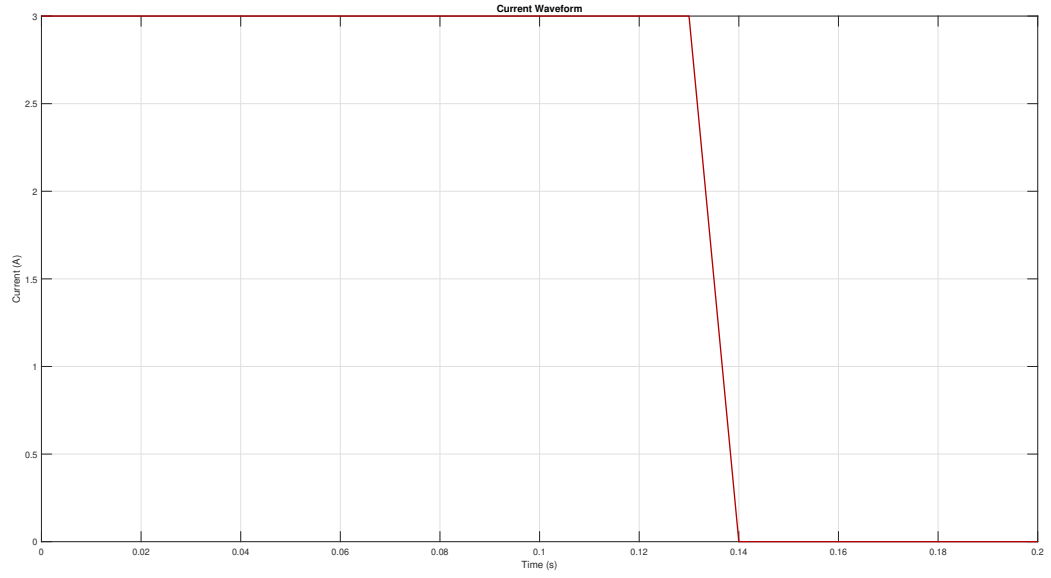


Figure 17: Current in controlled continuous rotation of nonlinear system

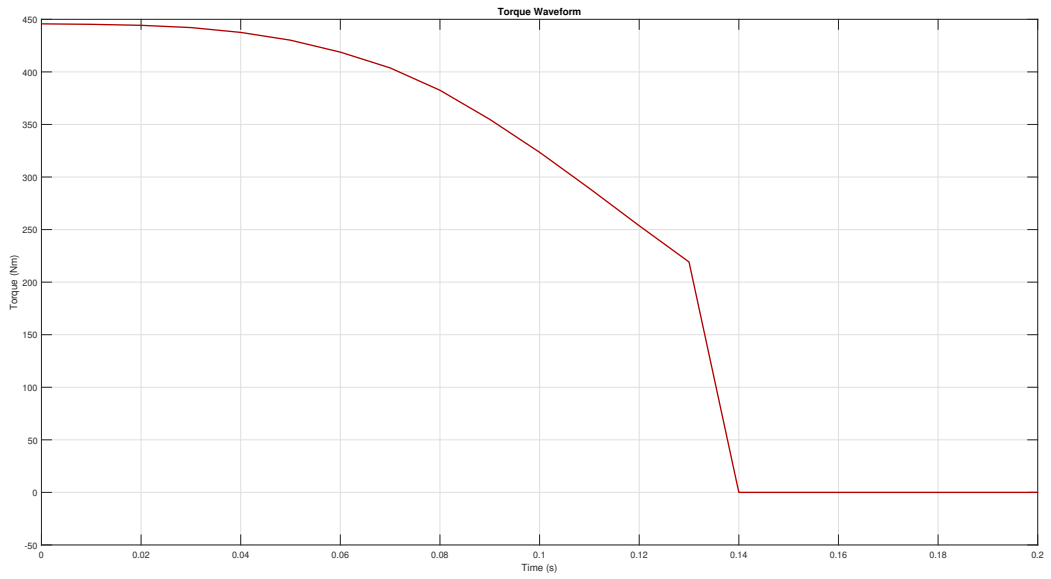


Figure 18: Torque in controlled continuous rotation of nonlinear system

Note that methodology is based on the position control, i.e., by controlling the position excitation currents are assigned. As can be seen from the Figs. 15-18, torque never decreases to negative values. The continuous rotations of the systems can be also seen in **animations**.

6 Motion Animation

The animations for both linear and nonlinear systems can be seen in the repository under **"Animations"** folder.

7 3D FEA Analysis

3D FEA model is created but due to hardware issues, I cannot run it, because it takes approximately 29 hours to run the simulation. Simulation model can be seen in repository.

8 Conclusion

Throughout this project, a basic reluctance machine is analyzed analytically and computationally. The results of the FEA models and analytical results are compared and presented. To conclude with, it is seen that analytical results are closer in linear FEA. In nonlinear FEA analysis, effect of leakage and fringing flux is observed, i.e., it is seen that inductance is increased due to fringing flux. Also, stored magnetic energy increases in nonlinear system since the area in the left hand side of the B-H curve increases, as expected. To sum up, analyzing with FEA gives more realistic result with appropriate modelling of the system.